



Optimization-based Process Synthesis for Sustainable Power Generation

Alexander W. Dowling, Lorenz T. Biegler*

Chemical Engineering Department, Carnegie Mellon University, Pittsburgh, PA 15213, USA
biegler@cmu.edu

Advanced power generation processes are challenged by needs for minimization of CO₂ emissions, higher energy efficiency and integration of superior processing technologies. These challenges also require the development of more effective models and strategies for large-scale process optimization. This study considers optimization tools and formulations for process synthesis, which highlight equation oriented modelling environments, nonsmooth modelling via complementarity conditions and fast optimization algorithms. We especially focus on novel formulations for process synthesis that take advantage of these state of the art optimization algorithms. All of these are formally represented as bi-level nonlinear programming (NLP) problems and include Gibbs reactor models, vapour-liquid equilibrium with vanishing and reappearing phases, and simultaneous heat integration and flowsheet optimization. These applications are demonstrated on the process synthesis of a coal oxycombustion process for clean electric power generation.

1. Introduction

Process synthesis strategies systematically explore nearly uncountable process configurations. Whether based on graphical representations, rule-based algorithms or optimization formulations, the goal of process synthesis is the selection of the best designs, with reduced costs, increased efficiency or improved operability. Ultimately, process engineers need to synthesize and optimize an entire process flowsheet with sufficiently detailed models. Unfortunately, many commercial simulation tools still struggle with full flowsheet optimization, thus restricting the size and scope of synthesis problems that can be practically considered. Even with state of the art simulation packages (e.g., AspenPlus, gPROMS, ProSIM, Pro/II) that offer gradient-based optimization, the structure of the flowsheeting model typically limits the formulation of nonlinear optimization problems to no more than 100 degrees of freedom.

While integration of nonlinear optimization presents demanding challenges for simulation tools, many of the capabilities for large scale optimization are available already in optimization modeling tools such as GAMS, AMPL and AIMMS. Moreover, during the last 20 years, additional families of NLP algorithms, such as interior point methods have been developed that are better suited for large optimization problems. These algorithms are not available in most commercial flowsheet simulators, as the optimization models require fully open, equation-oriented (EO) models with exact first and second derivatives. Large-scale NLP algorithms such as CONOPT, IPOPT, KNITRO and LOQO have been tailored to exploit these characteristics and lead to very fast performance for NLPs with many thousands of variables and degrees of freedom. Moreover, the extension of these optimization models for mixed integer nonlinear programming (MINLP), global optimization or optimization under uncertainty (through robust optimization or stochastic programming) all but requires a fully open optimization modeling environment. Moreover, results from an optimization study are more than 'just a number.' Characterizing the stability (uniqueness, curvature, ill-conditioning) of the problem, sensitivity to disturbances, model parameters and imposed inputs, and analysis of constraint activity are essential to understand, modify and apply the optimal solution. Efficient execution of this analysis can be done with efficient NLP sensitivity capabilities that are enabled by fast solvers with exact first and second derivatives (Pirnay et al., 2012).

The availability of such optimization capabilities also allows the consideration of novel NLP formulations that frequently arise in process engineering. In this study we focus on applications of bi-level NLPs for process synthesis. Such problems present a number of mathematical challenges but they are extremely useful for optimization-based process synthesis models. Examples for flowsheet synthesis include Gibbs reactor models that provide general behaviours of complex reactor systems, phase equilibria extended to disappearance (and reappearance) of phases, especially in vapour liquid separations and heat exchanger, and heat integration formulations that are embedded as optimization problems. While these applications are well known (Clark and Westerberg, 1990) we stress that they can be modelled and further developed as efficient equation oriented bi-level optimization problems that can be transcribed as Mathematical Programs with Complementarity Constraints (MPCCs). Solving these MPCCs is now possible with efficient NLP formulations and algorithms.

Moreover, the application of MPCC models is especially useful for process synthesis of advanced energy systems. Over the past decade tremendous opportunities have appeared for synthesis of advanced power systems that incorporate CO₂ capture and other metrics for sustainability. These can be handled naturally through optimization formulations and offer a wealth of applications for MPCC formulations. A particular application used in this study is the oxycombustion process, which serves as a motivating example for the demonstration of MPCC synthesis models. The remainder of the paper is organized as follows. Section 2 contains background information for the oxycombustion flowsheet including process component descriptions and design challenges. Section 3 then provides background of bi-level optimization problems and the reformation to MPCCs and NLPs. Section 4 outlines three applications of MPCCs, the Gibbs reactor, vapour liquid equilibria with phase disappearance and the embedded heat integration formulation. Section 5 provides an Air Separation Unit (ASU) synthesis case study, which demonstrates the performance of MPCC-based optimization. Finally conclusions and future work are discussed in Section 6.

2. The Oxycombustion Process

The impact of CO₂ emissions on climate change and the abundance of domestic coal resources motivate interest in “clean coal” technologies. Currently there are four popular methods of CO₂ abatement in coal power plants. The most direct method is post-combustion carbon capture, where CO₂ is separated from N₂ and other components in the fuel gas of a coal power plant. Captured CO₂ is pumped underground at high pressures for enhanced oil recovery and/or long term sequestration. The second approach, pre-combustion carbon capture, is specific to integrated gasification combine cycle (IGCC) power plants. Coal is first gasified to create syngas; next, the CO is shifted into CO₂; and finally the CO₂ is separated and sequestered. The remaining syngas (mainly H₂) is combusted to generate power and steam. In the third approach, chemical looping, oxygen is transported to the coal via a chemical carrier, such as a metal/metal oxide. This creates a CO₂ rich waste stream, which may not require an extensive separation step.

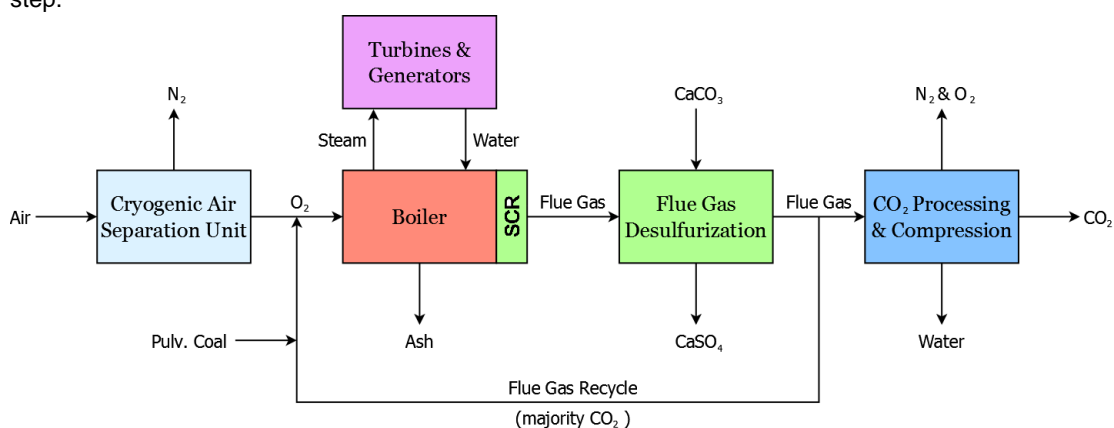


Figure 1: Simplified oxycombustion flowsheet

In the fourth approach, oxycombustion, coal is combusted in a N₂ lean environment. The resulting flue gas contains mainly water and CO₂, and requires significantly less processing before sequestration. Oxycombustion is also advantageous as it may be possible to retrofit existing coal and natural gas power plants with this technology. Figure 1 shows the four main components of the Oxycombustion flowsheet:

the air separation unit, the boiler coupled to the steam and power cycle, flue gas desulfurization and CO₂ processing and compression. First generation oxycombustion plants are expected to utilize cryogenic air separation units (ASU), where separation is achieved by distillation of air. At atmospheric pressure boiling points of N₂ and O₂ are -196 °C and -183 °C. These cold temperatures are achieved by compressing the inlet air, cooling it against exiting product streams in a multistream heat exchanger and then throttling the inlet air to a lower pressure, resulting in a temperature drop via the Joule-Thomson effect. Tight heat integration, with approach temperatures as small as 2 °C in the multistream heat exchanger, helps reduce energy consumption but greatly complicates design and optimization.

The oxygen from the ASU is then mixed with recycled flue gas (mainly CO₂ and water) and fed into the boiler, where pulverized coal is combusted. The recycle fraction is an important decision variable as the CO₂ diluent helps control the boiler temperature. Combustion of the coal produces heat, which is used to raise steam for power generation. Depending on coal quality, amount of N₂ in the boiler feed air, boiler design and flame temperature, varying amounts of NO_x and SO_x are formed. Evaluation of combustion properties for coal in a CO₂ - O₂ versus a traditional N₂ - O₂ environment remains an active area of research and accurate performance models for CO₂ - O₂ boilers are still under development.

Steam from the boiler is converted to mechanical and electrical power by steam turbines and electric generators. Several configuration options for the steam turbines must be considered by the designer including back-pressure exhausting to medium pressure, extraction back-pressure exhausting to medium and low pressure and condensing. Steam may need to be extracted at medium and low pressures to meet demands of processing units in the power plant. Finally the mechanical loads and steam demands must match with the selected steam turbine configuration. If the flowsheet designs change dramatically, turbines also need to be redesigned.

Depending on the combustion conditions, recycle strategy and future sequestration regulations, SO_x and NO_x need to be removed from the flue gas stream to various trace levels. In pulverized coal power plants, SO₂ is typically removed with a wet or dry flue gas desulfurization unit. In this process limestone (CaCO₃) reacts with SO₂ to form CaSO₄ hydrate (gypsum) and CO₂. NO_x is typically removed using a selective catalytic reduction (SCR) unit, where ammonia (NH₃) reduces NO_x, producing N₂ and H₂O (Steam, 2005). Due to the flue gas recycle in an oxycombustion plant, NO_x, CO and SO₃ all experience reburn near the nozzles, which are the hottest part of the boiler (Hack, 2010). Engineers at Foster Wheeler have proposed using this reburn phenomenon to downsize the pollution control systems in certain oxyfuel plants (Seltzer, 2010).

Finally, the treated CO₂ rich flue gas is dried and compressed to high pressures (up to 150 atm) for utilization and/or sequestration. A multi-stage compressor train with inter-stage cooling is required for compression. Drying is typically done in two steps. First the flue gas is cooled, which knocks out most of the water. Next an absorption process (ex: glycol dryer) is used to remove the remaining water. The drying and SO₂ removal steps reduce pipeline corrosion from the acidic flue gas.

Due to the tightly integrated nature of the oxycombustion plant, rigorous process evaluation, optimization or intensification studies must consider the entire system. Optimizing a single section, such as the boiler or steam cycle, inadequately predicts potential improvements, as changing one section of the flowsheet will cascade to the others. Moreover, intensification options such as heat integration only yield their full benefit by considering multiple sections. For this reason the oxycombustion power plant provides an excellent demonstration problem for new mathematical formulations that enable full flowheet optimization.

3. Enabling Optimization Tools

For optimization-based process synthesis mixed integer nonlinear programming (MINLP) formulations lead to the most general description of process optimization problems. To solve these problems, nonlinear programming (NLP) formulations are usually solved at a lower level for fixed values of the discrete variables. Based on information from the NLP solution, a search of the discrete variables is then conducted at a higher level. On the other hand, the ability to deal with (some) discrete decisions within an "all-at-once" NLP formulation can be more efficient than nested MINLP strategies, particularly if many discrete decisions must be handled. This motivates the modeling of discrete decisions with complementarity constraints (CC). Complementarity problems arise in a large number of applications in engineering and economic systems. They include contact and friction problems in computational mechanics, equilibrium relations in economics, and a wide variety of discrete events in process systems. However, these mathematical programming formulations and related solution strategies are not yet fully developed in process engineering.

Complementarities also arise naturally in the solution of multi-level optimization problems. Such problems are members of a more general problem class called Mathematical Programs with Equilibrium Constraints (MPECs) (Luo et al., 1996). For bi-level optimization problems of the form:

$$\min f(x) \text{ s.t. } (x, y) \in Z, y = \arg \left\{ \min_{\bar{y}} \theta(x, \bar{y}), \bar{y} \in C(x) \right\} \quad (1)$$

we define Z and $C(x)$ as feasible regions for the upper and lower level problems, respectively, with $f(x, y)$ and $\theta(x, y)$ as objective functions for the upper and lower level problems, respectively. In particular, bi-level optimization problems can be reformulated as mathematical programs with complementarity constraints (MPCCs) by writing the optimality conditions of the inner optimization problem (especially if this problem is convex) as constraints on the outer problem. An MPCC takes the following general form:

$$\min f(x), \text{ s.t. } h(x, y, z) = 0, g(x, y, z) \leq 0 \\ 0 \leq x \perp y \geq 0 \quad (2)$$

where \perp is the complementarity operator which forces orthogonality of the nonnegative vectors x and y , with z as the remaining variables. The complementarity constraint in (2) implies the following: $x_i = 0$ OR $y_i = 0$, $x \geq 0$, $y \geq 0$, for each vector element i . Here the OR operator is inclusive as both variables may be zero. Alternately, the complementarity constraint may be written in several equivalent ways including:

$$\begin{aligned} \text{i)} \quad & x^T y = 0, x \geq 0, y \geq 0 \\ \text{ii)} \quad & x_i y_i = 0, x \geq 0, y \geq 0 \\ \text{iii)} \quad & x_i y_i \leq 0, x \geq 0, y \geq 0 \\ \text{iv)} \quad & \text{or even, } x_i - \max(0, x_i - y_i) = 0. \end{aligned} \quad (\text{CC})$$

These alternate forms are particularly useful when applying existing nonlinear programming (NLP) solution strategies to solve MPCCs.

On the other hand, MPCCs of the form (2) cannot be solved directly with most NLP solvers because the associated optimality conditions of (2) do not satisfy constraint qualifications and therefore lead to singular KKT conditions. Consequently, if no reformulation of an MPCC is made and the complementarity is represented by any of the above choices, the constraint multipliers will be non-unique and unbounded, with dependent constraints at every feasible point. Consequently, the following MPCC reformulations have been presented in (Biegler, 2010) and allow standard NLP solvers to be applied.

$$\min f(x), \text{ s.t. } h(x, y, z) = 0, g(x, y, z) \leq 0 \\ x_i y_i \leq \varepsilon, x, y \geq 0 \quad (3)$$

$$\min f(x), \text{ s.t. } h(x, y, z) = 0, g(x, y, z) \leq 0 \\ x^T y \leq \varepsilon, x, y \geq 0 \quad (4)$$

$$\min f(x), \text{ s.t. } h(x, y, z) = 0, g(x, y, z) \leq 0 \\ x_i y_i = \varepsilon, x, y \geq 0 \quad (5)$$

$$\min f(x) + \rho(x^T y), \text{ s.t. } h(x, y, z) = 0, g(x, y, z) \leq 0, x, y \geq 0 \quad (6)$$

For the first three, regularized formulations, the complementarity conditions are relaxed and the MPCC is reformulated in (3), (4) or (5) with a positive relaxation parameter ε . The solution of the MPCC, (x^*, y^*, z^*) , can be obtained by solving a series of relaxed solutions as ε approaches zero. Convergence properties of these NLP formulations have been analysed in Ralph and Wright (1999). In contrast to the regularized formulations (3)-(5), we also consider the exact penalty function shown in (6). Here the complementarity can be moved from the constraints to the objective function and the resulting problem is solved for a particular value of ρ . Moreover, if ρ is greater than some critical value, then the complementarity constraints will be satisfied at the solution under certain regularity conditions. In this case if problem (6) has a solution with $x^T y = 0$, then this corresponds to the solution of (2). Conversely, any solution of (2) also is a solution of (6) if ρ is sufficiently large.

MPCC formulation (6) has a number of advantages. Provided that the penalty parameter is large enough, the MPCC may then be solved as a single problem, instead of a sequence of problems. Moreover, problem (6) allows any nonlinear programming solver to be used to solve a complementarity problem, without modifying the algorithm to deal with the sequence for ε . Moreover, using (6), the penalty parameter can also be changed during the course of the optimization, for both active set and interior point optimization algorithms. Finally, a number of numerical comparisons were conducted between (3), (4), (5)

and (6) with both active set and interior point algorithms. These are summarized in Baumrucker et al. (2008) and indicate that MPCC reformulation (6) usually has the most efficient and robust performance. MINLP models have been widely used in optimization-based process synthesis (see Biegler et al., 1997), and binary variables are especially needed for structural decisions (such as flowsheet topology) and logical conditions. However, switching decisions that involve inclusive OR operators that can also be modelled through MPCCs. As derived above through bi-level optimization problems, complementarity problems can deal effectively with a number of process-specific switches including nonsmoothness in process correlations and piecewise-smooth equations, check-valves, overflow conditions, controller saturation and compressor kickbacks. In the next section we highlight three important applications of MPCCs for process synthesis.

4. MPCC Synthesis Models

4.1 Equilibrium based reactors: Oxyfuel Case Study

We begin with an embedded minimization problem for the Gibbs reactor for oxycombustion (Kamath, 2012; Meinel, 2012). The inputs to the oxycombustion reactor are coal, oxygen, and flue gas recycle. For this work, the 14 chemical species in this system are declared as either reactive components (RCOMP) or inerts (ICOMP), and also classified as gases (GCOMP) or solids (SCOMP) since the fugacity calculations for the species depend on the phase. Only argon and ash are inerts that do not participate in the reaction equilibria. The optimization formulation allows the constituent atoms in the incoming feed to reorient into various possible reactive molecular species present in the reactor outlet. The total Gibbs free energy of the system is given by:

$$G^t = \sum_{i \in RCOMP} n_i G_i^0 + RT \sum_{i \in RCOMP} n_i \ln(\hat{\phi}_i / \phi_i^0) \quad (7)$$

where RCOMP is the set of reactive molecular species and n_i are corresponding molar flowrates, n is total molar flowrate and T is the system temperature. We set the standard state for pure gases and solids to $\phi_i^0 = 1$ bar and the Gibbs free energy of formation at the standard state as $G_i^0 = \Delta G_i^0$. Also, the set of reactive solids components defined as RSCOMP include carbon and sulphur; they are assumed to exist as pure substances whose fugacities are unaffected by pressure and mixing, i.e., $\hat{\phi} = \phi_i^0, i \in RSCOMP$. For the gas phase, partial molar fugacities are given ideally as, $\hat{\phi}_i = y_i P, i \in RGCOMP$ and component flowrates are related to mole fractions by

$$y_i = n_i / \left(\sum_{i \in GCOMP} n_i \right), i \in RGCOMP$$

With these substitutions we obtain the total Gibbs free energy of the system, which is the objective function to be minimized:

$$G^t = \sum_{i \in RCOMP} n_i \Delta G_i(T) + RT \left[\sum_{i \in RGCOMP} n_i \ln \left(\frac{P}{\sum_{i \in GCOMP} n_i} \right) + \sum_{i \in RSCOMP} n_i \ln n_i \right] \quad (8)$$

where $\Delta G_i(T)$ is the Gibbs free energy of formation adjusted for temperature (see Kamath, 2012). This is subject to constraints on the atomic mass balance:

$$\sum_{i \in RCOMP} a_{ji} n_i = \sum_{i \in RCOMP} a_{ji} n_{i0}, j \in NELEM \quad (9)$$

where n_{i0} is the net moles of species i at the gasifier inlet, a_{ji} is the number of atoms of element j in a molecule of species i , and $NELEM$ is the set of elements in the system. The other constraints to be satisfied are component balances for inerts $n_i = n_{i0}, i \in ICOMP$ and nonnegativity for the outlet molar flows, $n_i \geq 0, i \in RCOMP$.

Although the Gibbs free energy minimization technique has been used in many applications, its use in coal combustion has not been reported in the open literature except for the use of the equivalent RGIBBS model from the Aspen Plus simulator. Our model differs from the RGIBBS model in the following ways. First, our reactor formulation is fully equation oriented (EO) and can be easily customized and extended. Also, allows addition of other equality and inequality constraints apart from the method of temperature approach. Finally, this equilibrium based reactors can be naturally incorporated within the bi-level optimization problem. The inner problem minimizes Gibbs free energy while the outer problems optimizes the entire flowsheet (minimize operating cost, etc.). This bi-level optimization

problem can be solved by embedding the KKT conditions from the inner problem as constraints in the outer problem. Writing the KKT conditions for the Gibbs minimization reactor model leads to the following relations:

$$\begin{aligned}
\Delta G_i(T) + RT \left[\ln \left(\frac{P}{\sum_{i \in RGCOMP} n_i} \right) + 1 - \frac{\sum_{j \in RGCOMP} n_j}{\sum_{i \in RGCOMP} n_i} \right] + \sum_{k \in NELEM} \lambda_k a_{k,i} - \mu_i &= 0, \quad i \in RGCOMP \\
\Delta G_i(T) + \sum_{k \in NELEM} \lambda_k a_{k,i} - \mu_i &= 0, \quad i \in RSCOMP \\
\sum_{i \in RCOMP} a_{ji} n_i &= \sum_{i \in RCOMP} a_{ji} n_{i0}, \quad j \in NELEM \\
n_i &= n_{i0}, \quad i \in ICOMP \\
0 \leq \mu_i \perp n_i &\geq 0, \quad i \in RCOMP.
\end{aligned} \tag{10}$$

where the complementarity conditions from the inner KKT system lead to an MPCC. Equations (10) are easily extended to include process constraints and restricted equilibria that allow the tuning of this reactor model to specific, complex reacting systems. For instance, through the addition of approach temperatures and restricted equilibrium constraints, Kamath (2012) showed that these models accurately predict the performance of commercial gasifiers for the IGCC process.

We now consider the optimization of the oxycombustion boiler augmented with a steam cycle and auxiliary systems. In the oxycombustion boiler coal is combusted in an oxygen and CO₂ rich environment, producing addition CO₂, trace pollutants and water. As a first approximation this boiler may be considered to operate at or near equilibrium. This allows for the bi-level optimization approach described above to be applied. The steam cycle is modelled in this demonstration problem using the formulation proposed by Bruno et al. (1998). In this model steam turbines are decomposed into a superstructure, allowing for several configurations (back-pressure exhausting to medium pressure, condensing, etc.) to be considered. The model also contains logic to assign each main auxiliary load and electric generators to a dedicated turbine section. Two auxiliary loads are considered using simplified models; work required for the CO₂ compression section of the flowsheet is estimated using the ideal gas law, and the ASU is modeled using a simplified energy correlation, given by $E_{ASU} = 0.4261 y_{O_2} - 0.1538$ (kWh/kg O₂), where $y_{O_2} \leq 0.97$ is the mole fraction of product oxygen. The superstructure for the steam cycle (without auxiliary loads) is shown in Figure 2. The MINLP model also allows for the extraction of steam of three pressure levels, also allows for simultaneous utility and process optimization. To demonstrate the capability of this framework, an MP pressure steam demand of 20 MW was specified.

Using the bi-level Gibbs reactor model, steam cycle superstructure and simplified auxiliary load correlations, the overall operating cost of the oxycombustion flowsheet was minimized for a specific coal composition and price. Overall this resulted in 1,440 variables (51 integer) and 1,284 constraints. The turbine operating modes selected by the optimizer (DICOPT & CONOPT) are shown in Table 1. This sample plant is specified to produce the 550 MW of electricity. An additional 15.2 MWe powers minor auxiliaries, such as the vacuum and feed water pumps. The optimizer elects to assign these loads to electricity (with an efficiency penalty) instead of connected them to a dedicated turbine section. The two largest auxiliaries, the ASU and CO₂ compressors are assigned to dedicated turbine sections, as expected. The second medium pressure turbine allowed for in the superstructure is not used, and thus would not be constructed.

Intuition suggests the ASU compressor power requirements are too large, perhaps by a factor of 2, which can be explained by over-simplifications in the model. The correlation used to predict ASU energy requirements based on O₂ purity is conservative by 10 - 20 %, especially compared to the detailed ASU optimization results discussed in Section 5. The steam cycle considered includes two turbine sections – high and medium pressure, whereas typical power plants use three turbine sections – high, intermediate and low pressure. Finally the steam cycle model does not include reheat or steam extraction for feed water heating. Both of these process integration features are standard in the power industry for increasing plant efficiency. As a result the designed power plant only has an efficiency of 35 % (assuming the ASU and CO₂ compressor work is instead converted to electricity). Typical sub- and supercritical coal power plants have efficiencies around 36 % and 39 % LHV, respectively (Black, 2010). For all of these reasons, the optimized oxycombustion flowsheet results are preliminary and need to be extended to optimization with energy integration.

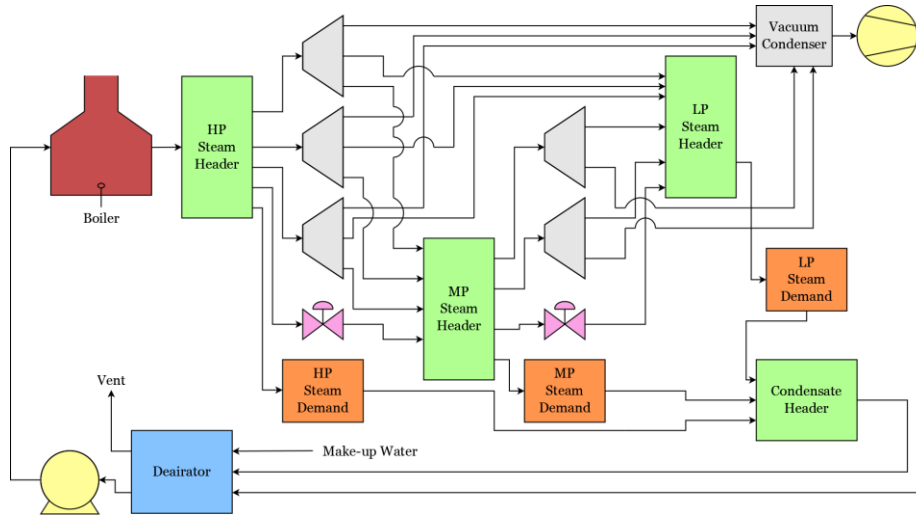


Figure 2: Steam cycle superstructure for demonstration problem

Table 1: Turbine Load Results

Turbine	Mode	Load	Work
High Pressure 1	Back-Pressure	Electricity Generator	39.0 MWe
High Pressure 2	Vacuum Condensing	Electricity Generator	526.2 MWe
High Pressure 3	MP Steam Extraction & Vacuum Condensing	ASU Compressor	230.1 MWe
Medium Pressure 1	Back-Pressure	CO ₂ Compressor	20.1 MWe
Medium Pressure 2	--	--	--

4.2 Flash models and extension to disappearing phases

In the equation-oriented model of the flowsheet, index sets organize the collection of streams and units. Streams contain properties (flowrates, temperature, enthalpy, etc) and units perform operations to change these stream properties. To exploit the features of these equation-oriented formulations and to demonstrate the ability of MPCC formulations to handle realistic vapour-liquid equilibrium models, we focus on an EO formulation for cubic equations of state (CEOS) a key relationship is given by:

$$f(Z) = Z^3 + aZ^2 + bZ + C \quad (11)$$

where Z is the compressibility factor and a , b and c are derived coefficients. Kamath et al. (2010) adapted CEOS for the EO formulation by adding inequality constraints to isolate values of Z corresponding to the liquid and vapour phases; these are given by:

$$f'(Z_L) = 3Z_L^2 + aZ_L + b \geq 0, \quad f''(Z_L) = 6Z_L - 2a \leq 0 \quad (12a)$$

$$f'(Z_V) = 3Z_V^2 + aZ_V + b \geq 0, \quad f''(Z_V) = 6Z_V - 2a \geq 0 \quad (12b)$$

Phase equilibrium is then calculated by relating the fugacity coefficients for liquid and vapour streams leaving every thermodynamic equipment unit as follows: $y_i/x_i = \phi(Z_L)/\phi(Z_V)$.

Over the course of the convergence path, changing pressures and temperatures will dictate whether process streams have one or two phases. When this happens the constraints specifying two-phase behaviour must be relaxed for the vanishing stream. This is accomplished through the addition of slack variables to the above inequalities, as discussed in Kamath et al. (2010). To illustrate, consider the Eq(13):

$$\begin{aligned}
F &= L + V \\
F z_i &= L x_i + V y_i, i \in N_c \\
F H_F + Q &= L H_L + V H_V \\
y_i &= \frac{\varphi(Z_L)}{\varphi(Z_V)} x_i, i \in N_c \\
f(Z_L) &= 0, f(Z_V) = 0
\end{aligned} \tag{13}$$

$$\begin{aligned}
F &= L + V \\
F z_i &= L x_i + V y_i, i \in N_c \\
F H_F + Q &= L H_L + V H_V \\
y_i &= \beta \frac{\varphi(Z_L)}{\varphi(Z_V)} x_i, i \in N_c \\
-s_L &\leq \beta - 1 \leq s_V \\
0 &\leq s_V \perp V \geq 0, 0 \leq s_L \perp L \geq 0 \\
f(Z_L) &= 0, f(Z_V) = 0 \\
f'(Z_L) &\geq 0, f'(Z_V) \geq 0 \\
f''(Z_L) &\leq M s_L, f''(Z_V) \geq -M s_V
\end{aligned} \tag{14}$$

which describes a simple PQ flash with CEOS. Here the triple (flow, mole fraction, enthalpy) applies to feed (F, z, H_F), liquid (L, x, H_L) and vapour products (V, y, H_V). By generalizing these equations through a Gibbs free energy minimization, Eq(13) can be reformulated (see Biegler, 2010) as a MPCC given in Eq(14). Note that as the slack variables s_L and s_V increase from zero, the liquid and vapour phases, respectively, are allowed to vanish. For this flash example we see that the inequality constraints that isolate the compressibility factors for each phase are relaxed and become redundant with disappearance of the phase. We also note that the equilibrium condition is relaxed with the addition of β . When one phase disappears β is relaxed from unity and the equilibrium constraint because inactive.

Since phase equilibrium model are ubiquitous in process models, the phase relaxation MPCC has a number of uses. MPCC formulations have been explored for a number of EO-based optimization problems including:

- NLPs formulations for distillation column design and simulation below the minimum reflux ratio (where trays dry up) (Raghuathan and Biegler, 2003)
- Heat integration with multistream, multi-stream heat exchangers, where phase determination is needed for over the length of the heat exchanger (Kamath et al., 2011)
- Startup of batch distillation columns while monitoring phase appearance and disappearance (Raghuathan et al, 2007)
- Optimal control of C3 separation with phase disappearance in reboilers (Fischer and Biegler, 2011)

In all of these cases, the MPCC, reformulated with the exact penalty function (6), effectively tracks the phase condition and leads to efficient and robust performance for the solution of large-scale NLPs.

4.3 Simultaneous Heat Integration and Process Optimization

Simultaneous optimization and heat integration of chemical processes was initially proposed by Duran and Grossmann (1986). In addition, Lang et al. (1988) and later Yee et al. (1990) improved this approach and expanded its application for flowsheet simulators and MINLP process design, respectively. This formulation can be derived from the well-known concepts of the Composite Curve method (see, e.g., Linnhoff, 1993) and the transshipment model (Papoulias and Grossmann, 1983), a linear program for targeting the minimum required utilities. Note that the heat exchange network is not considered directly in the simulation model described above. Instead, an optimization formulation related to optimal placement of the pinch curves (through the transshipment model) is used to model the integrated heat exchange system without having to impose a heat exchange network structure. However, embedding the LP directly within the NLP, or writing the corresponding optimality conditions as an MPCC, leads to a nonsmooth NLP. A complementarity representation along the lines of Eq(CC-iv) was developed by Duran and Grossmann (1986), along with a corresponding smoothing of the max operators. Following the approach of Duran and Grossmann (1986), the simultaneous process optimization and heat integration problem can be described as follows:

$$\begin{aligned}
&\min f(x) = \Phi(x) + c_s Q_s + c_w Q_w \\
&s.t. \quad h(x) = 0 \\
&\quad g(x) \leq 0 \\
&\quad Q_s \geq \sum_{j=1}^{n_c} f_j c_{p,j} [\max\{0, t_j^{out} - (T^p - \Delta T_{min})\} - \max\{0, t_j^{in} - (T^p - \Delta T_{min})\}] \\
&\quad \quad - \sum_{i=1}^{n_H} F_i C_{p,i} [\max\{0, T_i^{in} - T^p\} - \max\{0, T_i^{out} - T^p\}], p \in P \\
&\quad Q_w = Q_s + \sum_{i=1}^{n_H} F_i C_{p,i} (T_i^{in} - T_i^{out}) - \sum_{j=1}^{n_c} f_j c_{p,j} (t_j^{out} - t_j^{in})
\end{aligned} \tag{15}$$

where $\Phi(x)$ is the cost/profit function other than utility cost, Q_s is the requirement of the hot utility, Q_w is the requirement of the cold utility, $h(x)$ is the process flow sheet model, $g(x)$ represents the inequality constraints, j is the index for cold streams in the flow sheet, i is the index for hot streams, t_j is the temperature of cold stream j , T_i is the temperature of hot stream i , F_i and f_j are the heat capacity flowrates for the hot and cold streams, respectively. The index set P defines candidate pinch points from inlet temperatures of hot and cold streams; T^p , $p \in P$ is the candidate Pinch temperature defined as follows:

$$T^p = \begin{cases} T_i^{in} & \text{if candidate } p \text{ is hot stream } i \\ t_j^{in} + \Delta T_{\min} & \text{if candidate } p \text{ is cold stream } j \end{cases} \quad (16)$$

and ΔT_{\min} is the minimal temperature interval that is possible for the heat exchange to take place. The number of pinch temperature candidates is determined by the total number of hot and cold streams. The right hand sides of the inequalities for Q_s represent the difference between the heat contents of the cold and hot streams (heat deficit) above any candidate pinch. The problem is then posed to find the smallest value of Q_s such that all the inequalities hold; Q_s therefore equals the maximal value of the heat deficit and the temperature T^p where the heat deficit achieves this maximum is the pinch point.

The above formulation treats stream flows and temperatures as variables for both the optimization and the heat integration. For the nondifferentiable max operators in Eq(15) a smoothing approximation procedure can be used that avoids difficulties with the use of NLP solvers (see Biegler et al., 1997) as shown below:

$$\max\{0, \tau(x)\} = 0.5[\tau(x)^2 + \varepsilon^2]^{1/2} + 0.5\tau(x) \quad (17)$$

where ε usually assumes a relatively small value (e.g., 10^{-3} in our study). The optimization formulation (15) is applied to a number of ASU optimization cases in the next section. Each of these optimization problems was solved with the CONOPT solver in GAMS. As shown in the next section, because both solvers have access to exact first and second derivatives in an EO environment, optimization of all of these cases is obtained quite efficiently.

5. ASU Case Study

Optimization of a cryogenic air separation unit for the oxycombustion flowsheet is considered as a case study to demonstrate flash models with disappearing phases, cubic equation of state thermodynamics and heat integration with pinch curves. As discussed in section 4.1, an accurate ASU model is also required for reasonable full oxycombustion flowsheet optimization. Eventually these detailed ASU models will be combined with a revised version of the boiler and steam cycle model presented in section 4.1.

In the air separation unit, N_2 and O_2 are separated via distillation at cryogenic temperatures. This is typically done with coupled double column design, as shown in Figure 3. Feed air is compressed, cooled and split between the two columns. High purity N_2 is produced at the top of the high-pressure column. The bottoms, medium purity O_2 , are throttled down in pressure and recycled to the low-pressure column. The tops of the low pressure column are crude N_2 and the bottoms are high purity O_2 . The columns are tightly heat integrated to increase energy efficiency. The product streams are used to cool the feed stream with a multistream heat exchanger, represented by the many heat exchangers in Figure 3. Typically the low-pressure column reboiler also acts as the heat sink for the high pressure condenser. The coldest part of the column is typically the high purity N_2 after being throttled to ambient pressure. For the optimization formulation heat integration is considered using the models discussed in Section 4.3.

Design of the air separation unit is formulated as the following optimization problem:

min	Compression Energy	(kWh/kg O_2)
s.t.	CEOS Thermodynamics	(Section 4.2)
	Unit Operation Models	(Section 4.2)
	Heat Integration Model	(Section 4.3)
	Cascade Model	
	O_2 purity ≥ 90 mol%	

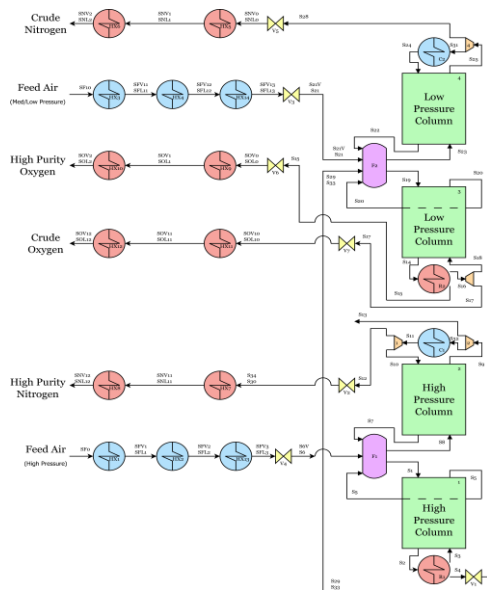


Figure 3: ASU Superstructure

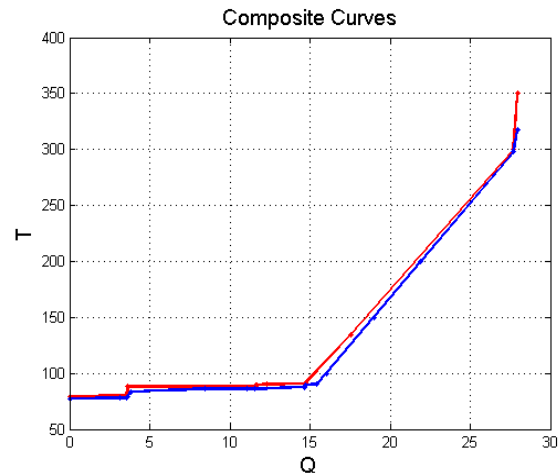


Figure 4: Composite Curves for Heat Integration

The unit operation models (flash, valve, reboiler, heat exchanger, etc) are extensions of the flash models presented in section 4.2. Final optimization is done using the cubic equation of state models discussed in section 4.2. Individual pairing of heat exchangers are not directly considered in this formulation. Instead the pinch location model presented in Section 4.3 is used. To accommodate nonlinearities in heat capacity due to phase changes, multiple heat exchangers in series are used with phase conditions fixed in some cases. For example, for the series of three heat exchangers used to cool the feed, air enters as a vapour and leaves as a liquid. The slack variables in (14) are specified such that the exit of the first heat exchanger is a saturated vapour. The exit of the second heat exchanger is a saturated liquid, along with the exit of the third heat exchanger (either saturated or subcooled liquid). This ensures phase transitions are isolated at the entrance and exit of the heat exchangers and eliminates the major concern with the constant heat capacity assumption in the heat integration.

Two different distillation cascade models are considered for ASU optimization. The first model is based on the work of Kamath et al (2010), which extends the group methods of Kremser and Edmister to a generic distillation cascade. The idea behind the group method is to approximate the cascade using a performance equation related to phase equilibrium in which the number of trays is a continuous variable. This is in contrast to the mixed integer nonlinear programming (MINLP) distillation models proposed by Viswanathan and Grossmann (1993). The group method approximation eliminates integer variables and greatly simplifies the optimization problem. After optimization is completed with the group method models, the results are used to initialize a rigorous tray-by-tray equilibrium distillation (MESH) model with a fixed number of stages. Optimization is repeated with the second model for the distillation cascades.

Using these models (with 6,887 variables and 7,170 constraints) the ASU compression energy was minimized and the best designs require compression energy of 0.18-0.2 kWh/(kg high purity O₂ product). This is comparable to other columns published in literature. For the best design the low-pressure column contains 21 stages and operates at 1.2 bar. The high-pressure column contains 42 stages and operates at 3.0 bar. Composite Curves resulting from the heat integration model (using the constraints from Duran and Grossmann (1986)) are shown in Figure 4. These curves show no external heating or cooling is required and the heat integration is very tight with multiple pinch points. As the ASU design problem contains highly nonlinear and ill-conditioned functions, a systematic initialization procedure has been developed that uses a simple thermodynamic model (correlations of vapour pressure, heats of vaporization, etc) to initialize the CEOS model. Likewise the group method cascade model results are used to initialize the more rigorous MESH model. We expect the ASU optimization results to improve, as model development and reformulation continues to lead to more robust initialization and reduced ill-conditioning. This approach contrasts with popular system analysis conducted commercial simulators. For example, in Jones et al (2011) several configurations were explored for an air separation for an IGCC coal power plant. For each configuration the flowsheet was “manually optimized” by varying flowsheet options. Instead, our approach considers systematic simultaneous optimization and flowsheet convergence. Also, with complementarity constraints, complex design challenges (phase disappearance, heat integration) are considered as part of the optimization problem, and advanced algorithms allow for the ASU to be converged *and* optimized in 3

CPU min on an Intel i5 laptop. This is the same order of magnitude of time required to only converge a single medium size flowsheet in a typical process simulator. Furthermore the results produced from the optimization approach lead to a guaranteed optimum with KKT conditions converged to a small tolerance. In contrast, “manually optimized” designs are limited by the designer’s time or convergence difficulties with the simulator. Finally the MPCC optimization approach also provides sensitivity information for the optimum with respect to parameters, disturbances and changing process requirements. Obtaining this information is not straightforward with a “manual optimization” procedure.

6. Conclusions

Advanced energy systems that meet the challenges of minimum CO₂ emissions, while maintaining high performance and efficiency, represent a new opportunity for process synthesis. Moreover, the availability of fast large-scale optimization tools and modeling environments leads to the development of efficient and powerful optimization-based process synthesis strategies. This study deals with the formulation and large-scale solution of bi-level optimization problems, posed as MPCCs. For process synthesis we explore three general applications. First, we consider Gibbs minimization reactor models to the design and operating space for the synthesis of complex reaction systems including combustion and gasification units. Next, we explore the fundamental application of phase equilibrium to develop more general models that include variable numbers of phases. With this extension we can expand the decision space for separation, heat transfer and a variety of stream conditions. Finally, we consider the incorporation of heat integration as a synergistic component of the overall process optimization problem. Developed from the well-known Duran-Grossmann formulation, this approach offers an optimal balance at the process synthesis stage between capital and operating expenses, energy consumption, CO₂ emissions and product sales.

Several improvements are already planned for the methods presented in this paper. For the ASU case study, model reformulation is underway to improve robustness. One approach that will be explored is to formulate the heat integration problem as an MPCC in the form of (6). This should remove some very small elements from the Jacobian and Hessian caused by the smoothed max operator (17), possibly improving the robustness of the initialization routine and leading to better local solutions. Other reformulations involving the CEOS equations are currently being explored. Extension of the ASU superstructure to include configurations popular in literature, such as ones presented by Jones et al (2011), is also planned. This will allow for more realistic ASU designs to be considered, leading to future energy improvements. Finally capital costs will be added to the ASU optimization problem.

With regard to the work presented in Section 4.1, two major improvements are planned. The first is development of a more sophisticated boiler model that considers materials (temperature) limits of heat transfer zones, radiative heat transfer and limited reaction kinetics. Revisions of the steam cycle are also underway. These include that addition of intermediate turbines, realistic turbine efficiency expressions, options for multiple reheats and steam extraction for boiler feedwater heating.

The equilibrium-based reactor model and flash calculations from Sections 4.1 and 4.2 are also being used to model auxiliary systems such as the SO_x scrubber and CO₂ processing and compression step. Eventually the improved ASU model, new boiler model, advanced steam cycle model and auxiliary models will be combined for optimization of the entire oxycombustion power plant, in order to extend and improve the preliminary results shown in Section 4.1. This large optimization problem will include the heat integration models from Section 4.3. Considering the entire flowsheet simultaneously will enable oxycombustion system to be holistically optimized and balance the trade-offs between each system. Our large-scale optimization approach also provides a systematic framework to evaluate heat integration opportunities throughout oxycombustion flowsheet, e.g., integrating pre- and post-combustion cryogenic systems. Finally, the many promising outcomes from this work include estimates of the potential for coal oxycombustion to economically produce reduced carbon electricity, which could guide policy makers.

Acknowledgement

Disclaimer: This article was prepared as an account of work sponsored by an agency of the United States Government. Neither the United States Government nor any agency thereof, nor any of their employees, makes any warranty, express or implied, or assumes any legal liability or responsibility for the accuracy, completeness, or usefulness of any information, apparatus, product, or process disclosed, or represents that its use would not infringe privately owned rights. Reference herein to any specific commercial product, process, or service by trade name, trademark, manufacturer, or otherwise does not necessarily constitute or imply its endorsement, recommendation, or favoring by the United States Government or any agency

thereof. The views and opinions of authors expressed herein do not necessarily state or reflect those of the United States Government or any agency thereof.

References

- Baumrucker B.T., Renfro J.G., Biegler L.T., 2008, MPEC problem formulations and solution strategies with chemical engineering applications, *Comput. Chem. Eng.* 32, 2903-2913
- Biegler L.T., Grossmann I.E., Westerberg A.W., 1997, *Systematic Methods for Chemical Process Design*, Prentice Hall, Upper Saddle River, NJ, USA
- Biegler L.T., 2010, *Nonlinear Programming: Concepts, Algorithms and Applications to Chemical Processes*, SIAM, Philadelphia, USA.
- Black J., 2010, *Cost and Performance Baseline for Fossil Energy Plants Volume 1: Bituminous Coal and Natural Gas to Electricity*, DOE/NETL Technical Report 2010/1250, Morgantown, WV USA
- Bruno J.C., Fernandez F., Castells F., Grossmann I.E., 1998, A rigorous MINLP model for the optimal synthesis and operation of utility plants, *Chem. Eng. Res. Des.* 76, 246-258
- Clark P.A., Westerberg A.W., 1990, Bi-level programming for steady state chemical process design, *Comput. Chem. Eng.* 14, 87-97
- Duran M.A., Grossmann I.E., 1986, Simultaneous Optimization and Heat Integration of Chemical Processes. *AIChE J.* 32, 123-140
- Fischer G.A., Biegler L.T., 2011, Fast NMPC Applied to Industrial High Purity Propylene Distillation, paper 140b, Annual AIChE Meeting, Minneapolis, MN USA
- Jones D., Bhattacharyya D., Turton R., Zitney S.E., 2011, Optimal design and integration of an air separation unit (ASU) for an integrated gasification combined cycle (IGCC) power plant with CO₂ capture Fuel Process. *Technol.* 92, 1685-1695.
- Hack H., Fan Z., Seltzer A., 2010, Advanced Oxyfuel Combustion Leading to Zero Emission Power Generation. 35th Int'l Conference on Clean Coal & Fuel Systems. Paper 120, Clearwater, FL USA
- Kamath R., 2012, PhD Thesis, Chem. Eng. Dept, Carnegie Mellon University, Pittsburgh, PA USA
- Kamath R. S., Grossmann I.E., Biegler L.T., 2010, Aggregate models based on improved group methods for simulation and optimization of distillation systems, *Comput. Chem. Eng.*, 34, 1312-1319
- Kamath R.S., Biegler L.T., Grossmann I.E., 2012, Modeling Multi-stream Heat Exchangers with Phase Changes for Simultaneous Optimization and Heat Integration, *AIChE J.* 58, 190-204
- Kamath R.S., Biegler L.T., Grossmann I.E., 2010, An equation-oriented approach for handling thermodynamics based on cubic equation of state, *Comput. Chem. Eng.* 34, 2085-2096.
- Lang Y.D., Biegler L.T., Grossmann I.E., 1988, Simultaneous Optimization and Heat Integration with Process Simulators, *Comput. Chem. Eng.* 12, 311
- Linnhoff, B., 1993 Pinch analysis - A state-of-the-art overview, *Trans. IChemE.*, 71(A), 503.
- Luo Z.-Q., Pang J.-S., Ralph D., 1996, *Mathematical Programs with Equilibrium Constraints*. Cambridge University Press, Cambridge, UK
- Meinel D., Modelling of an Oxy-fuel Process, 2011, Student Project Report, Chem. Eng. Dept., Carnegie Mellon University/TU Munich, Pittsburgh, PA, USA
- Papoulias S.A., Grossmann I.E., 1983, A structural optimization approach in process synthesis, *Comput. Chem. Eng.* 7, 695-706
- Pirnay H., Lopez-Negrete R., Biegler L.T., 2012, Optimal Sensitivity Based on IPOPT, *Math. Prog. Comp.*, 4, 307-331
- Raghunathan A.U., Biegler L.T., 2003, MPEC Formulations and Algorithms in Process Engineering. *Comput. Chem. Eng.* 27, 1381-1392
- Raghunathan A., Diaz M.S., Biegler L.T., 2004, An MPEC Formulation for Dynamic Optimization of Distillation Operation, *Comput. Chem. Eng.* 28, 2037-2052
- Ralph D., Wright S.J., 1999, Some Properties of Regularization and Penalization Schemes for MPECs. *Opt. Meth. Soft.* 19, 527-556
- Seltzer A., Fan Z., Hack H., Shah M., 2010, Simulation of Pollutants in Flexi-Burn, Oxyfuel Pulverized Coal Power Plant. 35th Int'l Conf. on Clean Coal & Fuel Systems, Paper 105, Clearwater, FL, USA
- Steam: Its Generation and Use, 2005, The Babcock and Wilcox Company, Columbus, OH, USA
- Viswanathan J., Grossmann I. E., 1993, Optimal Feed Locations and Number of Trays for Distillation Columns with Multiple Feeds, *Ind. Eng. Chem. Res.* 32, 2942-2949
- Yee T.F., Grossmann I.E., Kravanja Z., 1990, Simultaneous Optimization Models for Heat Integration. III., *Comput. Chem. Eng.* 14, 1185-1200